Disruption, segregation, and passivation for Pd and noble-metal overlayers on $YBa_2Cu_3O_{6.9}$

T. J. Wagener, Y. Gao, I. M. Vitomirov, C. M. Aldao, J. J. Joyce, C. Capasso, and J. H. Weaver
Department of Chemical Engineering and Materials Science, University of Minnesota, Minneapolis, Minnesota 55455

D. W. Capone II
Materials Science Division, Building 223, Argonne National Laboratory, Argonne, Illinois 60439
(Received 27 January 1988)

We have investigated interfaces formed when Pd and the noble metals Cu, Ag, and Au are deposited onto polycrystalline samples of $YBa_2Cu_3O_{6.9}$ fractured in an ultrahigh vacuum. Synchrotron-radiation photoemission results show that Cu and Pd overlayers leach oxygen from the underlying $YBa_2Cu_3O_{6.9}$ substrate, disrupt the superconductor, and destroy electronic states near the Fermi level. Interface reactions become kinetically limited at room temperature after the deposition of ~4 Å of Cu or Pd, significantly sooner than for the reactive metals Fe, Al, Ti, and In. The presence of Ba near the surface after the deposition of more than 100 Å of Cu and Pd reflects substrate disruption and subsequent surface segregation. In contrast, overlayers of Ag and Au do not disrupt the superconductor substrate, no segregation is observed, but the overlayers are nonuniform and the quality of passivation is in question for coverages <100 Å.

INTRODUCTION

The discovery of materials that exhibit superconductivity at temperatures above 77 K (Refs. 1 and 2) has resulted in a frenzy of activity. Much of the scientific interest has sought a better fundamental understanding of the physical mechanisms responsible for the high critical temperature T_c and manipulation of the parameters so that T_c can be pushed even higher. Scientific and technical efforts have also focused on developing devices based on these materials or integrating them into existing technologies.

The electronic structures of these ceramic superconductors have been examined by many workers using photoelectron spectroscopy[3-7] (PES), inverse photoelectron spectroscopy[3,8] (IPES), and band-structure calculations.[9,10] All agree that the valence bands are dominated by hybrid Cu–O bonds. The stability[8,11] and interfacial properties[4,12-14] of $La_{1.85}Sr_{0.15}CuO_4$ and $YBa_2Cu_3O_{6.9}$ have also been investigated with electron spectroscopies and the techniques of surface science. Such investigations have shown, for example, that Au passivates the $La_{1.85}Sr_{0.15}CuO_4$ surface.[13] In technological applications, it has been observed that Ag and Au are effective metals to use at contacts with $YBa_2Cu_3O_{6.9}$, but fundamental studies of surface reactions have not been reported.

In this paper, we report the results of synchrotron radiation photoemission investigations of microscopic interactions that occur when adatoms of Pd, Cu, Ag, and Au are deposited under ultrahigh vacuum conditions onto fractured surfaces of $YBa_2Cu_3O_{6.9}$. We have exploited the tunability of the synchrotron light source to emphasize changes in spectral features for the Cu 3*d* satellites, the Ba 5*p* shallow core levels, the states near the Fermi level, and the overlayers. Interest in Cu overlayers reflects the importance of Cu in current-carrying technologies and the fact that it is one of the constituents in the 1:2:3 and 2:1:4 ceramic superconductors. Great interest in Ag and Au results from their stability against oxidation. Palladium was studied because of its near-noble metal character. Our studies have shown that both Cu and Pd leach oxygen from the substrate while Ag and Au form nonreactive, nonuniform overlayers. For Cu and Pd, reactions at the surface become diffusion limited as the developing metal oxides act as barriers against oxygen loss.

EXPERIMENT

The photoemission experiments were conducted at the Wisconsin Synchrotron Radiation Center using the 800-MeV Aladdin ring. The facility 3-m toroidal grating monochromator and beamline provided photons in the range $10 \leq h\nu \leq 135$ eV. The high-energy cutoff imposed by the optics of the beamline provided a fortuitous rejection of second-order radiation in studies of the Cu valence-band satellites with $70 \leq h\nu \leq 80$ eV. Photoelectron energy discrimination was done with a double-pass cylindrical-mirror analyzer operating at a pass energy of 18 eV. The overall resolution in the energy distribution curves (EDC's) ranged from 0.2 eV at $h\nu = 40$ eV to 0.5 eV at $h\nu = 135$ eV.

The $YBa_2Cu_3O_{6.9}$ samples were high-density, polycrystalline posts with superconducting transition temperatures of ~92 K.[15] These ~4×4×12 mm posts were fractured *in situ* at pressures of 8×10^{-11} Torr and all measurements were performed at room temperature. Detailed XPS core-level analysis of these samples showed that the fractured surfaces were at least as good as those prepared by scraping, as judged by the amount of Ba, C, and O emission representative of residual impurities. [A discussion of these x-ray photoemission spectroscopy (XPS) comparisons for a wide range of samples will be given by Meyer *et al.*[4]] Overlayers of the metals were deposited via standard evaporation from resistively heated W boats. The amount of material deposited was determined with a

quartz thickness monitor. Stable evaporation rates were established before the samples were exposed to the sources for the appropriate lengths of time. The typical deposition rate was ~1 Å/min and the pressure in the experimental chamber was below 2×10^{-10} Torr during evaporation. Depositions, Θ, are reported in angstrom units based on the density of the bulk metals. They represent the amount of material deposited rather than the thickness of the overlayer since the latter cannot be known, particularly when reaction is observed. Data acquisition time for each EDC was ~5 min.

RESULTS AND DISCUSSION

Cu/$YBa_2Cu_3O_{6.9}$—disruption and segregation

In Fig. 1, we summarize the valence-band emission for the Cu/$YBa_2Cu_3O_{6.9}$ interface as measured with a photon energy of 50 eV. The bottom curve for the freshly prepared surface shows the valence bands to be dominated by Cu $3d$-O $2p$ hybrid bands that extend from the Fermi level, E_F, to ~8 eV below E_F. The states at E_F are derived from the antibonding Cu $3p_{x^2-y^2}$-O $2p_{x,y}$ levels[9,10] and are presumed to play a crucial role in superconductivity. Emission from them can be seen to be very low, a fact supported by inverse photoemission (IPES) spectra which show the top of the Cu–O band to extend to ~1.5 eV above E_F. (The Y $4d$, Ba $5d$, and Ba $4f$ states lie farther above E_F.[8]) The remaining Cu–O bands show a dominant peak at 4.8 eV and a shoulder at 2.3 eV below E_F. It is likely that part of the strength of the 4.8 eV structure is due to residual contamination present in all of the samples studied to date, as suggested by Miller, Fowler, Brundle, and Lee[5] and Fujimori, Takayama-Muromachi, Uchida, and Okai.[6] Indeed, in the very recent investigations of single crystals, Stoffel *et al.*[7] showed a line shape with more weight on the leading edge at 2.3 eV and less at 4.8 eV. Finally, Fig. 1 shows a prominent feature 9.1 eV below E_F. Although it has been observed in every low-energy photoemission study of these materials, its origin remains the source of continuing discussion. In general, very similar spectra have been observed in almost all of the photoemission studies of fractured or scraped surfaces.

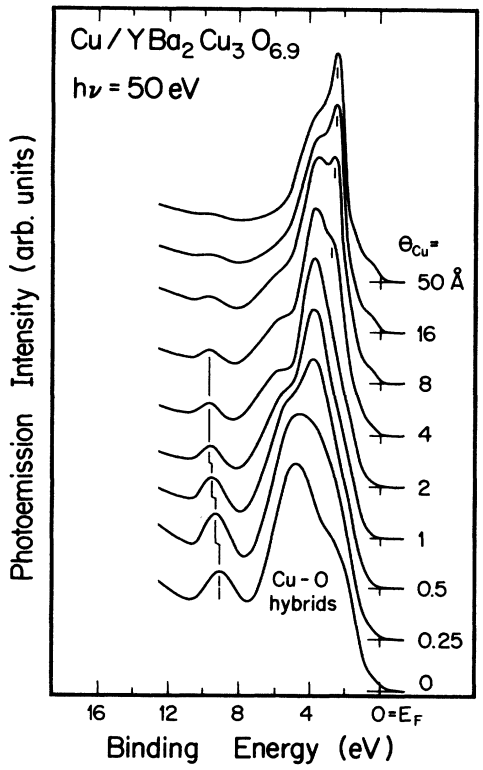

FIG. 1. Synchrotron radiation photoemission spectra for Cu/$YBa_2Cu_3O_{6.9}$ using $h\nu=50$ eV. The spectra are normalized to constant peak height for visual clarity. The loss of emission near E_F signifies surface disruption. Ultimately, a metallic Cu overlayer starts to form at a Cu coverage of 4 Å, as indicated by the sharp Fermi level.

In Fig. 1, the EDC's offset upward show the effects of Cu depositions from 0.25–50 Å. For visual clarity, they have been normalized to constant height. The deposition of even small amounts of Cu reduces the total emission close to E_F, and this suppression suggests the destruction of superconductivity in the region probed by our measurements. The reduced emission at E_F is apparent for $\Theta_{Cu}=0.25$, 0.5, 1, and 2 Å. Thereafter, a well-defined Fermi-level cutoff reappears as the metallic Cu contribution near E_F becomes apparent. The valence band develops further and shows the characteristic line shape of Cu metal with a dominant maximum at 2.4 eV. By $\Theta_{Cu}=16$ Å, its shape is indistinguishable from that of Cu metal, except for a small feature at ~9.8 eV.[16] A similar scenario of interface disruption, followed by eventual Cu film growth, has been reported for Cu/$La_{1.85}Sr_{0.15}CuO_4$ based on XPS and IPES studies.[14] These studies showed that the loss of emission at E_F is accompanied by the conversion of Cu from a nominal 2^+ to a 1^+ valence and changes in the binding energy of the O $1s$ core levels.

To investigate the changing Cu bonding configurations during interface evolution, we examined the Cu final-state satellite structures in the valence band. This is done best through resonance enhancement of the Cu-derived features using a photon energy of ~76 eV.[17] In the right half of Fig. 2 we show the energy region from 6 to 20 eV below E_F where the Cu d^8 final-state satellite features are clearly visible at 12.4 eV and, less clearly, at ~10.0 eV. (The latter is obscured by the larger feature at 9.1 eV.) As can be seen, the deposition of up to 1 Å of Cu leads to the rapid loss of the d^8 satellite feature and the growth of a new feature at 15.4 eV. This corresponds to the conversion of Cu^{2+} to Cu^{1+} throughout the probed region since the feature at 15.4 eV is due to the Cu d^9 final state of Cu_2O.[18] Moreover, it shows that the adatoms of Cu react with O to form the Cu^{1+} valence state. For depositions greater than ~2 Å, we see another change in the satellite features. The vertical lines in Fig. 2 draw attention to the growth of structure at 14.2 and 11.5 eV. These reflect the nucleation and growth of Cu metal with final-state configuration d.[10] Spectra taken with $h\nu=73$ eV verified that these features were indeed Cu satellites since their

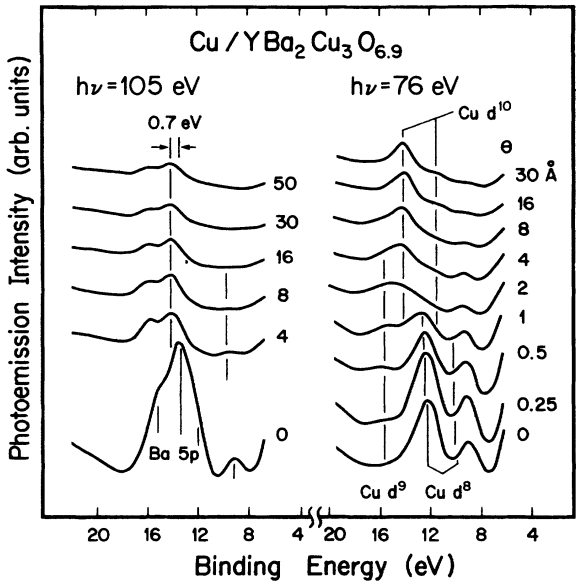

FIG. 2. Resonant photoemission spectra for $Cu/YBa_2Cu_3O_{6.9}$. The right panel shows the enhanced Cu d^8 (12.4 and -10.0 eV), d^9 (15.4 eV), and d^{10} (14.2 and 11.5 eV) final-state satellites. These three Cu configurations reflect the Cu valence state in the superconductor, the thin Cu_2O interlayer, and metallic Cu. The left panel displays the enhanced Ba 5p features. The 0.7-eV shift of the Ba 5p levels reflects the destruction of the Ba phase which appears in the superconductor (lower binding-energy shoulder).

emission intensities diminished markedly.[17,18]

The extremely rapid disappearance of the Cu d^8 satellite illustrates that all of the Cu–O bonds of the divalent form are destroyed in the outermost 10–15 Å of our superconducting substrate by the deposition of only 2 Å of Cu (probe depth is three times the mean free path). If we assume that each Cu atom in the superconductor substrate relinquishes an average of 0.5 O atoms to form the Cu_2O overlayer, then a 2-Å Cu deposit would scavenge O from $\sim$10 Å of the ceramic. We consider 10–15 Å to be a lower limit for substrate modification because Cu 2p XPS studies, with a greater probe depth of $\sim$50 Å, showed complete Cu valence change for $Cu/La_{1.85}Sr_{0.15}CuO_4$.[14] With additional depositions of Cu onto this modified interfacial region, the Cu d^9 satellite emission was gradually attenuated and disappeared by $\Theta = 16$ Å when only the Cu d^{10} satellite features can be observed (Fig. 2). Since the Cu d^9 satellite disappears, we conclude that a rather uniform metallic overlayer forms on the Cu_2O interlayer. Although we have no direct electrical measurements for these interfaces, we suspect that the result is a complex, high-resistance contact between Cu and the buried superconductor.

To determine whether the Cu-derived layer effectively covered the surface, we investigated the Ba 5p emission as a function of Cu deposition. In the left panel of Fig. 2, we show the resonantly enhanced Ba 5p features for selected depositions using $h\nu = 105$ eV. (It is a consequence of resonance photoemission that changing the photon energy makes it possible to suppress or enhance the spectral features of Ba relative to the Cu satellite even though they appear at very nearly the same energy.) The apparent Ba $5p_{3/2}$ maximum is at 13.7 eV while the $5p_{1/2}$ is at 15.4 eV for the freshly cleaved surface (bottom left EDC). This Ba 5p feature is composed of contributions from Ba in the chemical environment representative of the superconductor and those from chemically shifted residual BaO, $Ba(OH)_2$, and $BaCO_3$ located in the exposed grain boundaries of our polycrystalline sample.[4,5] Detailed analysis of the multiple Ba phases presented by Meyer *et al.*[4] and Miller *et al.*[5] showed that the contaminant Ba phases have higher binding energies and that the lower binding-energy

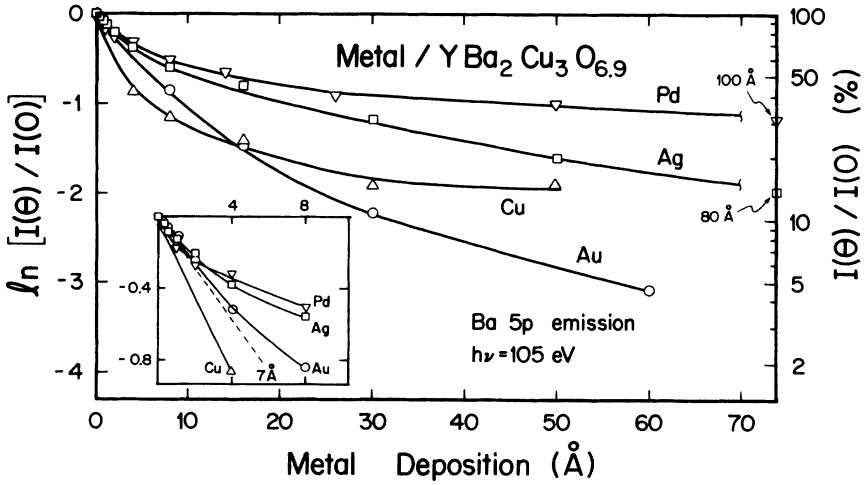

FIG. 3. Attenuation curves representing the normalized integrated emission from the Ba 5p features as a function of Cu, Pd, Ag, and Au coverage $\ln[I(\Theta)/I(0)]$. The dashed line indicates the behavior expected for layer-by-layer growth. Barium atoms segregate to the surface for Pd and Cu overlayers, as reflected by the almost flat attenuation curves for $\Theta > 30$ Å. For Ag and Au, deviations reflect inhomogeneous growth.

shoulder represents Ba in the ceramic superconductor. Unfortunately, the Ba content of these contaminant phases is larger than that of the superconductor and emission from exposed intergranular Ba overwhelms emission from Ba exposed by transgranular fractures.

The deposition of 4 Å of Cu produces a sharper Ba $5p$ doublet that appears shifted 0.7 eV to higher binding energy with respect to the cleaved surface. Significantly, the shoulder representative of the Ba bonding configuration in the superconductor is lost. This loss provides additional evidence for substrate destruction and shows the changing chemical environment for Ba. It is also interesting to note that, although the Cu_2O interlayer was covered by $\Theta_{Cu}=16$ Å, the Ba emission persists after $\Theta_{Cu}=50$ Å. This is consistent with inverse photoemission results where Ba emission persisted past $\Theta_{Cu}=500$ Å.[19] These facts hint that Ba segregates to the surface of the growing metallic overlayer. Comparison of the final energy and splitting (Ba $5p_{1/2,3/2}$ doublet at 16.3 and 14.5 eV) with the results of Ref. 20 suggests that these Ba atoms are in an oxide form.

To further characterize interface evolution, we present in Fig. 3 the integrated Ba $5p$ emission normalized to the clean surface emission $\ln[I(\Theta)/I(0)]$ as a function of overlayer deposition for Cu, Pd, Ag, and Au. The total Ba $5p$ intensities were obtained after subtraction of a linear background and corrections for changes in photon flux. For Cu overlayers, there is an initial rapid attenuation that is consistent with a photoelectron mean free path of ~7 Å. At higher coverage, the rate of attenuation is much slower, suggesting either poor covering up of the surface or Ba segregation. Since the Cu d^9 valence-band satellite attenuated at a rate consistent with layer-by-layer growth, we conclude the Ba segregates to the surface region of the thickening Cu film. Moreover, the very small decrease in the Ba emission at high coverage indicates that it continues to float and the solubility of Ba in Cu is very small. This is consistent with the presence of Ba at $\Theta_{Cu}=500$ Å, as reported by inverse photoemission.

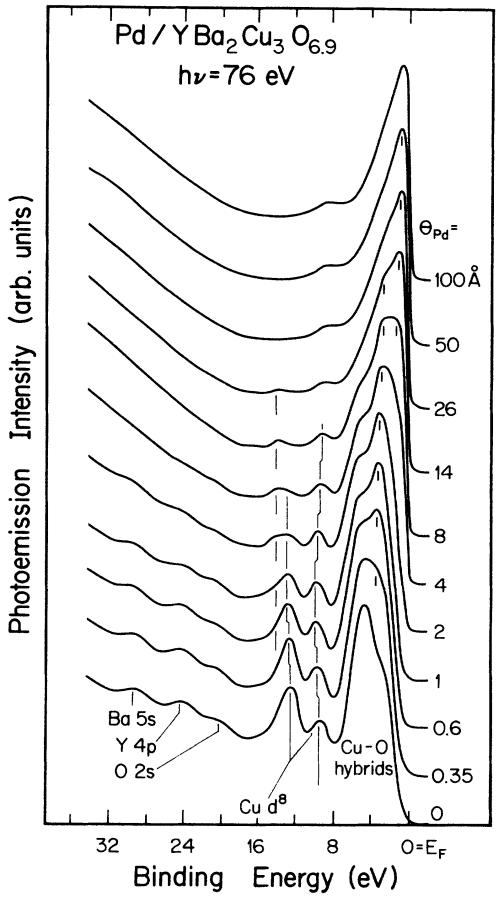

FIG. 4. Valence-band spectra ($h\nu=76$ eV) for $Pd/YBa_2Cu_3O_{6.9}$. The destruction of the states near E_F reflects the growth of PdO at the expense of the substrate. The loss of the resonantly enhanced Cu d^8 satellite after $\Theta_{Pd}=4$ Å suggests the destruction of superconductivity in the near-surface region. For $\Theta_{Pd}>26$ Å, only metallic Pd valence-band features can be seen.

$Pd/YBa_2Cu_3O_{6.9}$—disruption and segregation

In Fig. 4, we show the evolving valence-band spectra for the $Pd/YBa_2Cu_3O_{6.9}$ interface taken at a photon energy of $h\nu=76$ eV to emphasize the Cu d^8 satellite features. Again, we see that the substrate emission near E_F is reduced by metal adatom deposition, especially between 0.35 and 2 Å; this is more obvious in spectra taken at $h\nu=50$ eV spectra, as in Fig. 1 for Cu. We attribute this reduction to the disruption of Cu—O hybrid states as oxygen is withdrawn from the near-surface region to form Pd—O. Emission from this Pd—O reaction product has a distinct valence-band feature at 3 eV (tic marks). When $\Theta_{Pd}=4$ Å, there is the reappearance of emission at E_F and we associate this with the nucleation of Pd metal. Thereafter, there is a steady increase in the characteristic Pd-derived peak centered at 0.6 eV and the valence-band spectra are indistinguishable from metallic Pd by $\Theta_{Pd}=50$ Å.[21] It is also interesting to note that the authors of Ref. 21 found a reduction in the Pd-derived 0.6-eV peak when clean Pd was exposed to oxygen.

The results of Fig. 4 show the loss of all of the valence-band features other than those of Pd, suggesting that a rather uniform Pd overlayer has formed. This can be seen most graphically from changes in the Cu d^8 satellite at 12.4 eV since it is well isolated from the dominant states near the Fermi level. With Pd deposition, it declines rapidly in intensity, disappearing by $\Theta_{Pd}=8$ Å. There is also a total shift of 0.3 eV to higher binding energy, a shift which was also found for Cu overlayers. This reflects subtle changes in Cu ion final-state screening associated with variations in environment and oxygen depletion. Unfortunately, we know of no studies of the d^8 satellite as a function of oxygen stoichiometry within the nominal Cu^{2+} configuration, although the numerous XPS investigations of different superconductor samples show $2p$ satellites of varying intensities.[6] When the Cu satellite is lost by conversion of the Cu^{2+} configuration, we find a feature appearing at ~14 eV. This feature grows to a peak between $\Theta_{Pd}=2$ and 4 Å, and thereafter attenuates and disappears by 26 Å.

More detailed insight into the evolving Ba environments

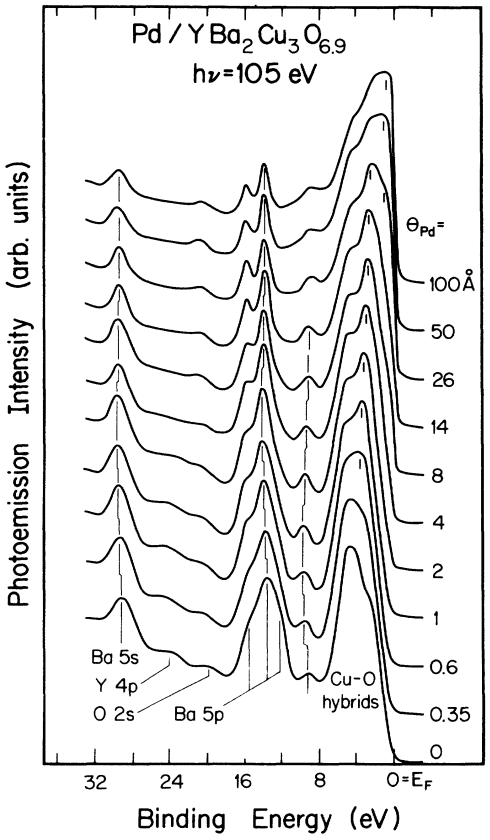

FIG. 5. EDC's for $Pd/YBa_2Cu_3O_{6.9}$ which emphasize the Ba features. The initial sharpening and shift to higher binding energy reflects the destruction of the low-binding-energy shoulder which is attributed to Ba in the superconductor. For $\Theta_{Pd} > 4$ Å, the Ba features sharpen and shift to lower binding energy because of surface segregation of elemental Ba.

can be obtained from the resonantly enhanced Ba 5*p* and 5*s* features shown in Fig. 5. As noted above, Ba is present at the freshly prepared surface in several bonding configurations. The multiphase Ba 5*p* and Ba 5*s* features identified in Fig. 5 sharpen with Pd deposition and shift 0.7 eV to higher binding energy upon the deposition of only $\Theta_{Pd} = 1$ Å. At higher coverage, the Ba features return 0.4 eV to lower binding energy and become considerably sharper, with no change observed after $\Theta_{Pd} = 26$ Å. In-depth analysis of the Ba 5*s* emission showed that Pd deposition quickly diminishes the low-binding-energy component and the peak position appears at 0.7 eV higher binding energy. The full width at half maximum (FWHM) decreases from 2.5 eV for the fresh surface to 2.0 eV at $\Theta_{Pd} = 4$ Å. We interpret these changes as reflecting the initial disruption of the superconductor, which destroys the Cu satellite and changes the Ba environment in the depleted superconductor. Ba is still present in its nonsuperconductor environment, as well as the contamination phase. Thereafter, the Ba 5*s* emission shifts to lower energy by 0.4 eV and sharpens to 1.6 eV, close to that found for metallic Ba. Concurrently, the Ba 5*p* emission sharpens and stabilizes with a splitting of 2 eV. We speculate that after the initial surface disruption, the metallic Pd overlayer uniformly covers the interface but that elemental Ba segregates to the surface. Such segregation would then be analogous to that frequently observed at metal/semiconductor interfaces involving reactive metal overlayers.

The surface segregation of Ba for Pd overlayers is further indicated by our attenuation curve in Fig. 3. The attenuation of the total Ba 5*p* signal has a 1/*e* length of ~260 Å for $\Theta_{Pd} > 26$ Å, as shown in Fig. 3. This extremely slow attenuation would be characteristic of Ba segregation on the surface. Although it might also reflect clustering or a nonuniform Pd overlayer, the absence of emission from other substrate components for $\Theta_{Pd} = 100$ Å argues against such nonuniformities. Moreover, since the Cooper minimum for Pd 4*d* electrons occurs at ~120 eV,[22] our results at $h\nu = 105$ eV would be very sensitive to Cu 3*d* states at ~2.5 eV. Since our valence-band spectra near E_F stabilize by $\Theta_{Pd} = 50$ Å to a shape very similar to that found by Ref. 23 for Pd, and there is no obvious sign of Cu 3*d* contribution, we conclude that the Pd overlayer is quite uniform and the Ba signal at $\Theta_{Pd} = 100$ Å is due to surface segregation.

Ag/$YBa_2Cu_3O_{6.9}$ and Au/$YBa_2Cu_3O_{6.9}$—passivation

Of all the interfaces studied to date with $YBa_2Cu_3O_{6.9}$, the only ones which do not exhibit reaction of the sort just described are those based on Ag and Au. The results, summarized in Fig. 6, show that the states at the Fermi

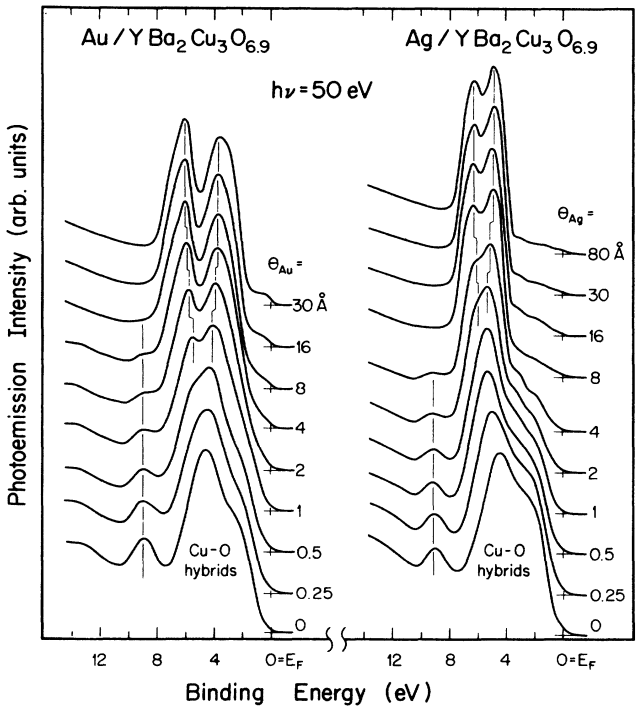

FIG. 6. Valence-band spectra for $Ag/YBa_2Cu_3O_{6.9}$ (right panel) and $Au/YBa_2Cu_3O_{6.9}$ (left panel). The states at E_F are not destroyed by Ag or Au, suggesting that superconductivity is not suppressed in our substrate. The results show the convergence of the Ag and Au *d* bands by 8 Å nominal coverage.

level are not destroyed by interaction with Ag and Au adatoms. Instead, the Cu $3p_{x^2-y^2}$-O $2p_{x,y}$ emission remains almost constant as the overlayer simultaneously attenuates the substrate and contributes its own *sp*-derived states. By coverages of ~8 Å, the distinctive Ag and Au line shapes near E_F have developed. The relative emission at E_F for our metallic Ag or Au overlayers is rather low since $h\nu = 50$ eV is near the peak in the photoionization cross section for the Au 5*d* and Ag 4*d* levels.[24] Likewise, the valence-band splitting of the Ag and Au *d* bands, which increases as the layer thickness increases, becomes stable at coverages of ~8 Å. This is consistent with what is found for Au deposited onto nonreactive graphite substrate.[25] We conclude that there is little intermixing or surface reaction. This is supported by the fact that the feature at 9.1 eV shows no chemical shift of the sort observed for the reactive Cu and Pd overlayers.

Examination of the resonantly enhanced Cu d^8 satellite shown in the right panels of Fig. 7 indicates that the satellite remains stationary and clearly visible for Ag and Au depositions of 8 Å. Unfortunately, there is a broad $5p_{1/2}$ *VV* Auger feature for Au that appears with a kinetic energy of ~54 eV. This grows with coverage and partially obscures the Cu d^8 satellite. Nonetheless, the results of Fig. 7 show strong evidence for its existence at $\Theta_{Au} = 30$ Å. Since the results for Ag are free of this complication, it is possible to detect the satellite to $\Theta_{Ag} = 80$ Å. In the left panels of Fig. 7 we show the evolving Ba 5*p* region, again using resonance photoemission to enhance the Ba contribution. The invariance in binding energy suggests that the chemical environments of Ba did not change. However, Ba emission persisted to coverages of Θ_{Au} ~60 Å and Θ_{Ag} ~80 Å, suggesting that both Au and Ag cover the substrate nonuniformly. Similar results have been reported for the Au/$La_{1.85}Sr_{0.15}CuO_4$ interface where clusters were shown to form at low coverages and eventually coalesced at coverages in excess of 100 Å.[13]

Line-shape analysis of the Ba 5*p* and 5*s* emission suggests that the Ba phases are covered at different rates. The low-binding-energy components characteristic of the superconductor are attenuated more rapidly than the contamination components. For Ag, the Ba 5*s* FWHM is reduced from 2.5–2.2 eV by the deposition of 80 Å due to the loss of emission from the superconductor component. This suggests that overlayer growth is more effective on the superconductor, but detailed discussions of surface mobility are impossible without suitable single crystals.

The attenuation of the Ba 5*p* feature for Au and Ag overlayers is shown in Fig. 3. The Au attenuation curve is nearly identical to that found for the Au/$La_{1.85}Sr_{0.15}CuO_4$ interface.[13] At high coverage, the 1/*e* lengths are ~26 Å in our study, compared to ~20 Å for Au/$La_{1.85}$-$Sr_{0.15}CuO_4$. This suggests that there is little or no Ba outdiffusion or segregation. We can speculate that at higher coverages (Θ_{Au} ~100–150 Å) the similarities will persist and that the clusters will coalesce to form a stable, protective overlayer. For Ag, the 1/*e* attenuation length is ~50 Å at high coverage. As for Au, we suggest that Ag clusters on the surface.

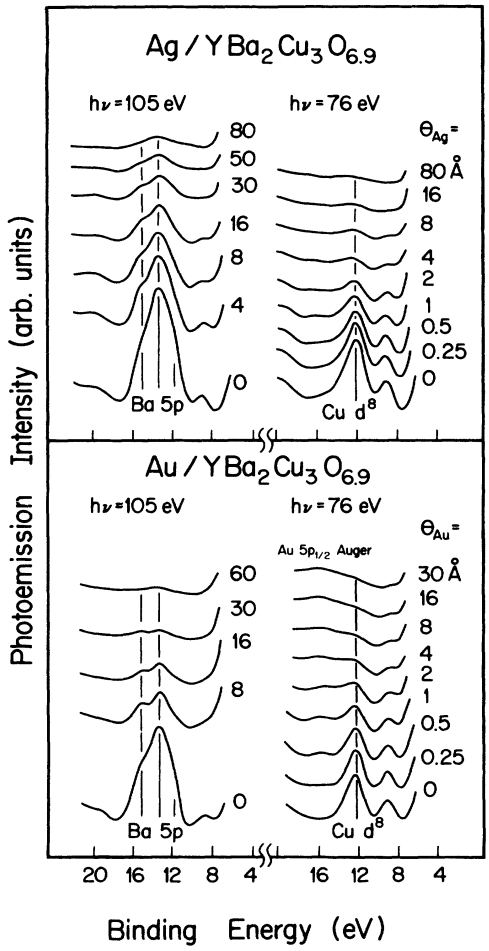

FIG. 7. The top panel shows the resonantly enhanced Cu d^8 satellite and Ba 5*p* feature for Ag/$YBa_2Cu_3O_{6.9}$. The bottom panel shows similar spectra for Au/$YBa_2Cu_3O_{6.9}$. These spectra show attenuation effects indicative of overlayer growth, with no signs of surface disruption.

CONCLUSIONS

We have shown that the deposition of Cu and Pd onto $YBa_2Cu_3O_{6.9}$ is disruptive. The destruction of the hybrid Cu–O bonds and the changes in the core-level emission indicate changes in chemical bonding and almost certainly signifies the loss of superconductivity in the near-surface region. However, metallic layers of Cu and Pd appeared at nominal coverages of ~4 Å. This suggests that the interface reactions are kinetically limited at room temperature. Comparison of these results to those for Fe, Al, Ti, and In showed that the disruption caused by Cu and Pd was much less than the others. Indeed, interface reactions were not kinetically limited until coverages of ~24 Å for Fe, ~14 Å for Al, ~10 Å for Ti, and ~8 Å for In on $YBa_2Cu_3O_{6.9}$.[12] For depositions of ~50 Å of Cu and Pd, the overlayers were found to be nearly uniform with a substantial amount of segregated Ba from our disrupted interface region. The interfaces formed by Au and Ag on $YBa_2Cu_3O_{6.9}$ are significantly different than those involving Pd and Cu since there is no evidence for reaction.

This suggests that superconductivity in the near-surface region would not be affected. However, for Au and Ag coverages of ~4 to ~100 Å, we observe the overlayers to be nonuniform.

As we have emphasized in the text, the existence of intergranular contaminants has complicated the interpretation of the data. Nevertheless, we are able to identify spectroscopic features of the superconductor. By following these features during the interface formation, we eliminated the influence of the contaminants and deduced pictures of interface formation of the noble metals (Cu, Ag, Au) and the near noble metal (Pd) with the high-T_c superconductor $YBa_2Cu_3O_{6.9}$.

Note added in proof. Our more recent studies with metal overlayers on single crystals of 1:2:3 and 2:1:4 superconductors support these conclusions while giving more precise information about the intrinsic properties of the clean surfaces.

ACKNOWLEDGMENTS

The work at Minnesota was supported by the University of Minnesota, the Office of Naval Research under Grant No. ONR N00014-87-K-0029, and an IBM Materials Science and Processing grant. The work at Argonne National Laboratory was supported by Department of Energy under Grant No. W-31-109-Eng-38. The photoemission experiments were done at the National Science Foundation-supported Wisconsin Synchrotron Radiation Center and the assistance of its staff is gratefully acknowledged.

[1]J. G. Bednorz and K. A. Müller, Z. Phys. B **64**, 189 (1986).

[2]C. W. Chu, P. H. Hor, R. L. Meng, L. Gao, Z. J. Huang, and Y. Q. Wang, Phys. Rev. Lett. **58**, 405 (1987).

[3]There have been many photoemission studies. See, for example, *Thin Film Processing and Characterization of High-Temperature Superconductors-1987,* edited by J. M. E. Harper, R. F. Colton, and L. C. Feldman, Proceedings of the American Vacuum Society Special Conference on High-Temperature Superconductivity, AIP Conference Proceedings No. 165 (AIP, New York, 1988), and references therein; See also H. M. Meyer III, Y. Gao, T. J. Wagener, D. M. Hill, J. H. Weaver, B. K. Flandermeyer, and D. W. Capone II, *ibid.*, p. 254; P. Steiner, J. Albers, V. Kinsinger, I. Sander, B. Siegwart, S. Hufner, and C. Politis, Z. Phys. B **66**, 275 (1987); B. Reihl, T. Riesterer, J. G. Bednorz, and K. A. Müller, Phys. Rev. B **35**, 8804 (1987); N. Nücker, J. Fink, B. Renker, D. Ewert, C. Politis, J. W. P. Weigs, and J. C. Fuggle, Z. Phys. B **67**, 9 (1987); P. D. Johnson, S. L. Qiu, L. Jiang, M. W. Ruckman, M. Strongin, S. L. Hulbert, R. F. Garrett, B. Sinkovic, N. V. Smith, R. J. Cava, C. S. Jee, D. Nicols, E. Kaczanowicz, R. E. Salomon, and J. E. Crow, Phys. Rev. B **35**, 8811 (1987); R. L. Kurtz, R. L. Stockbauer, D. Mueller, A. Shih, L. E. Toth, M. Osofsky, and S. A. Wolf, *ibid.* **35**, 8818 (1987); P. Steiner, V. Kinsinger, I. Sander, B. Siegwart, S. Hufner, and C. Politis, Z. Phys. B **67**, 19 (1987); M. Onellion, Y. Chang, D. W. Niles, R. Joynt, G. Margaritondo, N. G. Stoffel, and J. M. Tarascon, Phys. Rev. B **36**, 819 (1987); J. A. Yarmoff, D. R. Clarke, W. Drube, U. O. Karlsson, A. Taleb-Ibrahimi, and F. J. Himpsel, *ibid.* **36**, 3967 (1987); P. Steiner, V. Kinsinger, I. Sander, B. Siegwart, S. Hufner, C. Politis, R. Hoppe, and H. P. Müller, Z. Phys. B **67**, 497 (1987); T. Takahashi, F. Maeda, H. Arai, H. Katayama-Yoshida, Y. Okabe, T. Suzuki, S. Hosoya, A. Fujimori, T. Shidara, T. Koide, T. Miyahara, M. Onoda, S. Shamoto, and M. Sato, Phys. Rev. B **36**, 5686 (1987).

[4]H. M. Meyer III, D. M. Hill, T. J. Wagener, Y. Gao, J. H. Weaver, D. W. Capone II, and K. C. Goretta, Phys. Rev. B (to be published).

[5]D. C. Miller, D. E. Fowler, C. R. Brundle, and W. Y. Lee, in *Thin Film Processing and Characterization of High-Temperature Superconductors,* Ref. 3, p. 336.

[6]A. Fujimori, E. Takayama-Muromachi, Y. Uchida, and B. Okai, Phys. Rev. B **35**, 8814 (1987).

[7]N. G. Stoffel, Y. Chang, M. K. Kelly, L. Dottl, M. Onellion, P. A. Morris, W. A. Bonner, and G. Margaritondo, Phys. Rev. B **37**, 7952 (1988).

[8]Y. Gao, T. J. Wagener, J. H. Weaver, A. J. Arko, B. Flandermeyer, and D. W. Capone II, Phys. Rev. B **36**, 3971 (1987); T. J. Wagener, Y. Gao, J. H. Weaver, A. J. Arko, B. K. Flandermeyer, and D. W. Capone II, *ibid.* **36**, 3899 (1987).

[9]L. F. Mattheiss, Phys. Rev. Lett. **58**, 1028 (1987); Jaejun Yu, A. J. Freeman, and J.-H. Xu, *ibid.* **58**, 1035 (1987); L. F. Mattheiss and D. R. Hamann, Solid State Commun. **63**, 395 (1987); R. V. Kasowski, W. Y. Hsu, and F. Herman, *ibid.* **63**, 1077 (1987); T. Fujiwara and Y. Hatsugai, Jpn. J. Appl. Phys. **26**, L716 (1987); R. V. Kasowski, W. Y. Hsu, and F. Herman, Phys. Rev. B **36**, 7248 (1987); F. Herman, R. V. Kasowski, and W. Y. Hsu, *ibid.* **36**, 6904 (1987); W. M. Temmerman, G. M. Stocks, P. J. Durham, and P. A. Sterne (unpublished).

[10]F. Herman, R. V. Kasowski, and W. Y. Hsu, in *Novel Superconductivity,* edited by S. A. Wolf and V. Z. Kresin (Plenum, New York, 1987).

[11]T. J. Wagener, Y. Gao, H. M. Meyer III, I. M. Vitomirov, C. M. Aldao, D. M. Hill, J. H. Weaver, B. K. Flandermeyer, and D. W. Capone II, in *Thin Film Processing and Characterization of High-Temperature Superconductors,* Ref. 3, p. 368; N. G. Stoffel, J. M. Tarascon, Y. Chang, M. Onellion, D. W. Niles, and G. Margaritondo, Phys. Rev. B **36**, 3986 (1987).

[12]Y. Gao, H. M. Meyer III, T. J. Wagener, D. M. Hill, S. G. Anderson, J. H. Weaver, B. K. Flandermeyer, and D. W. Capone II, in *Thin Film Processing and Characterization of High-Temperature Superconductors,* Ref. 3, p. 358; J. H. Weaver, Y. Gao, T. J. Wagener, B. K. Flandermeyer, and D. W. Capone II, Phys. Rev. B **36**, 3975 (1987); D. M. Hill, H. M. Meyer III, J. H. Weaver, B. Flandermeyer, and D. W. Capone II, *ibid.* **36**, 3979 (1987); Y. Gao, T. J. Wagener, J. H. Weaver, B. K. Flandermeyer, and D. W. Capone II, Appl. Phys. Lett. **51**, 1032 (1987); H. M. Meyer III, D. M. Hill, Steven G. Anderson, J. H. Weaver, and D. W. Capone II, *ibid.* **51**, 1750 (1987); Y. Gao, T. J. Wagener, J. H. Weaver, and D. W. Capone II, Phys. Rev. B **37**, 515 (1988), Y. Gao, I. M. Vitomirov, C. M. Aldao, T. J. Wagener, J. J. Joyce, C. Capasso, J. H. Weaver, and D. W. Capone II, J. Appl. Phys. (to be published).

[13]H. M. Meyer III, T. J. Wagener, D. M. Hill, Y. Gao, S. G. Anderson, S. D. Krahn, J. H. Weaver, B. Flandermeyer, and

D. W. Capone II, Appl. Phys. Lett. **51**, 1118 (1987).
[14]D. M. Hill, Y. Gao, H. M. Meyer III, T. J. Wagener, J. H. Weaver, and D. W. Capone II, Phys. Rev. B **37**, 511 (1988).
[15]J. D. Jorgensen, H.-B. Schüttler, D. G. Hinks, D. W. Capone II, K. Zhang, M. B. Brodsky, and D. J. Scalapino, Phys. Rev. Lett. **58**, 1024 (1987).
[16]J. Stohr, F. R. McFeely, G. Apai, P. S. Wehner, and D. A. Shirley, Phys. Rev. B **14**, 4431 (1976).
[17]M. Iwan, F. J. Himpsel, and D. E. Eastman, Phys. Rev. Lett. **43**, 1829 (1979).
[18]M. R. Thuler, R. L. Benbow, and Z. Hurych, Phys. Rev. B **26**, 669 (1982).
[19]Y. Gao, T. J. Wagener, J. H. Weaver, and D. W. Capone II, inverse photoemission results for $Cu/YBa_2Cu_3O_{6.9}$ (unpublished).
[20]K. Jacobi, C. Astaldi, B. Fricle, and P. Geng, Phys. Rev. B **36**, 3079 (1987).
[21]H. Conrad, G. Ertl, J. Kuppers, and E. E. Latta, Surf. Sci. **65**, 245 (1977).
[22]J. W. Cooper, Phys. Rev. **128**, 681 (1962).
[23]S. Hufner and B. K. Wertheim, Phys. Lett. **47**, 349 (1974).
[24]J. J. Yeh and I. Lindau, At. Data Nucl. Data Tables **32**, 1 (1985).
[25]G. K. Wertheim, S. B. DiCenzo, and S. E. Youngquist, Phys. Rev. Lett. **51**, 2310 (1983).